UNVEILING CONTROL VECTORS IN LANGUAGE MODELS WITH SPARSE AUTOENCODERS

Anonymous authors
Paper under double-blind review

ABSTRACT

Sparse autoencoders have recently emerged as a promising tool for explaining the internal mechanisms of large language models by disentangling complex activations into interpretable features. However, understanding the role and behavior of individual SAE features remains challenging. Prior approaches primarily focus on interpreting SAE features based on their activations or input correlations, which provide limited insight into their influence on model outputs. In this work, we investigate a specific subset of SAE features that directly control the generation behavior of LLMs. We term these "generation features", as they reliably trigger the generation of specific tokens or semantically related token groups when activated, regardless of input context. Using a systematic methodology based on causal intervention, we identify and validate these features with significantly higher precision than baseline methods. Through extensive experiments on the Gemma models, we demonstrate that generation features reveal interesting phenomena about both the LLM and SAE architectures. These findings deepen our understanding of the generative mechanisms within LLMs and highlight the potential of SAEs for controlled text generation and model interpretability. Our code is available at https://anonymous.4open.science/r/control-vector-with-sae-AAFB.

1 INTRODUCTION

Large Language Models (LLMs) have demonstrated remarkable capabilities in natural language understanding and generation (Brown et al., 2020; Touvron et al., 2023; Jiang et al., 2023; Bai et al., 2023). However, their black-box nature poses significant challenges, such as hallucination, bias, and factual inconsistency (Ji et al., 2023; Chang et al., 2024; Huang et al., 2023). A key reason for these challenges lies in the way individual neurons within these models encode multiple, seemingly unrelated concepts, a phenomenon known as superposition (Elhage et al., 2022). This entanglement of features complicates efforts to isolate and manipulate specific generative behaviors.

Sparse Autoencoders (SAEs) have emerged as a promising tool to address this issue by disentangling mixed representations (Bricken et al., 2023; Huben et al., 2024). SAEs map dense model activations to sparse, interpretable latent spaces, revealing latent structures that explain LLM internals. However, prior approaches mainly interpret SAE features by analyzing activations or input correlations, providing limited insights into their impact on model outputs. This gap hinders the practical utility of SAEs for precise output control.

In this work, we investigate a specific subset of SAE features, which we term **generation features**. These features act as control vectors within the LLM, reliably triggering the generation of specific tokens or semantically related token groups when activated. Notably, their influence persists across different input contexts, indicating that these features encode information that directly drives the model's generative behavior. We propose a novel causal intervention-based methodology for systematically identifying generation features. Our approach involves activating individual SAE features and measuring their causal effects on token generation probabilities to pinpoint which feature consistently controls specific outputs. Through rigorous experiments, we demonstrate that our method achieves significantly higher precision in identifying these control vectors compared to baseline approaches, such as logit lens-based methods.

Based on our method, our study reveals that generation features are concentrated in specific model regions, particularly in deeper layers, aligning with the hierarchical organization of LLMs where

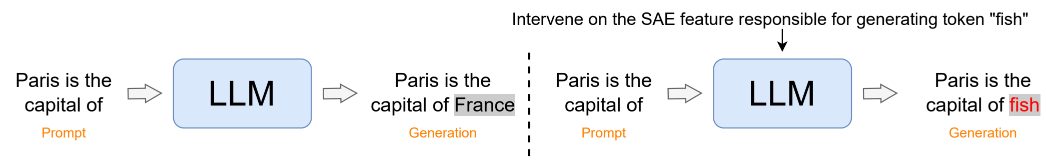

Figure 1: Illustration of generation features, which refers to specific learned features in a sparse autoencoder that contribute to the generation of certain tokens. On the left, the LLM generates the correct token "France" in response to the prompt "Paris is the capital of." On the right, an intervention is performed on the SAE feature responsible for generating the token "fish," which results in the LLM producing "fish" instead of "France." This highlights how specific features can influence the model's generation behavior in an expected way.

abstract and task-specific representations emerge. Additionally, we find that increased SAE sparsity enhances feature disentanglement and interpretability, while wider SAEs identify more features but at a lower relative density. Furthermore, by categorizing these features based on their generated outputs, we uncover patterns across token types, such as punctuation, common words, named entities, and programming-related tokens, providing insights into how LLMs organize generative knowledge through sparse, interpretable components.

Our contribution: (1) We introduce the concept of generation features, specific SAE features that reliably control token generation in LLMs. (2) We propose a novel causal intervention-based methodology to identify and validate these features with high precision. (3) Our analysis reveals that generation features are concentrated in specific model layers and are influenced by SAE design choices such as sparsity and width. (4) We categorize generation features based on their generated outputs, providing insights into the organization of generative knowledge in LLMs.

2 Related Works

Sparse Autoencoders and Feature Disentanglement. The phenomenon of superposition in neural networks, where individual neurons simultaneously encode multiple concepts (Elhage et al., 2022), has driven the development of sparse autoencoders (SAEs) for language model interpretation. Drawing from fundamental principles in sparse coding (Olshausen & Field, 1996), contemporary research demonstrates SAEs' capability to decompose complex representations in LLMs into interpretable features (Bricken et al., 2023; Huben et al., 2024). Bricken et al. (2023) demonstrated that stronger sparsity constraints lead to more monosemantic features, while Gao et al. (2025) introduced frameworks for scaling SAEs without compromising interpretability. Current approaches, however, predominantly analyze features through their activation patterns and input correlations, inferring feature concepts from activation circumstances (Huben et al., 2024). Consequently, the causal relationships between SAE neurons and model outputs remain insufficiently explored.

Controllable Text Generation. The field of controllable text generation has evolved along two primary trajectories. The first approach emphasizes decoding-time interventions, employing auxiliary networks to steer the generation process (Hu et al., 2017; Chen et al., 2019). The second operates within the latent space, beginning with efforts to learn disentangled representations during training (Hu et al., 2017; Chen et al., 2019) and progressing to recent methods for identifying and manipulating existing representations in pretrained models through steering vectors (Subramani et al., 2022; Rimsky et al., 2024). While these methods effectively control high-level generation aspects such as sentiment and topic, they primarily rely on aggregate representations or model-wide interventions. Our research advances this field by demonstrating that SAE-learned features naturally function as control vectors without requiring additional training or contrastive techniques. Moreover, our focus on individual SAE features' causal effects enables more precise control at the token and semantic concept level, leveraging the inherent disentanglement properties of these representations.

Causal Analysis in Neural Networks. Causal intervention frameworks (PEARL, 1995) have emerged as powerful tools for understanding information flow in transformers (Vig et al., 2020) and mapping knowledge representations (Meng et al., 2022). Although these investigations establish foundational methods for analyzing causal relationships in neural networks, they predominantly address broad architectural components or aggregate representations. Our methodology extends these foundations by applying causal abstraction techniques specifically to SAE features, capitalizing on their disentangled nature. This synthesis enables the identification of robust causal connections between individual features and specific outputs, overcoming the traditional challenges posed by representational superposition.

3 Preliminaries

3.1 Sparse Autoencoder

An activation vector a^j at layer j can be approximated as a linear combination of feature activations and their corresponding directions:

$$a^j \approx b + \sum_i f_i(a^j) d_i, \tag{1}$$

where b is a bias vector, $f_i(a^j)$ represents the activation of feature i, and each d_i is a unit vector in activation space representing the direction of feature i. To learn the feature activations f_i and feature directions d_i, we employ a sparse autoencoder. In this setup, the encoder maps the input activation a to a sparse code of feature activations:

$$f(a) = \sigma(W_e a + b_e), \tag{2}$$

where σ is a non-linear activation function, W_e is the encoder weight matrix, and b_e is the encoder bias. The decoder reconstructs the input activation from the sparse code:

$$\hat{a} = W_d f(a) + b_d, \tag{3}$$

where W_d is the decoder weight matrix whose columns d_i represent the feature directions, and b_d is the decoder bias. By training the autoencoder with a sparsity constraint on $f(a)$, we encourage the model to learn a set of meaningful features $\{d_i\}$ that can effectively reconstruct a from a sparse combination of feature activations.

3.2 Causal Intervention

In the context of neural networks, causal intervention involves modifying the internal activations to assess their causal impact on the model's output. Specifically, we intervene on the learned features $f(a)$ to observe how changes in feature activations affect the model's predictions. Using Pearl's do-operator (PEARL, 1995), we define an intervention that sets the feature activations to specific values:

$$do(f_i(a) = f'_i), \tag{4}$$

where f'_i is the intervened value of feature i. This allows us to study the causal effect of feature i on the model's output by comparing the predictions before and after the intervention.

4 Methodology

4.1 Model and Notation

Let M be a language model parametrized by a weight set θ that takes a tokenized prompt x as input and returns a probability distribution over the next token for all tokens in the vocabulary V of size N_V:

$$P_M(Y = y_i | x) = M(x; \theta)_i, \quad \forall i \in \{1, \ldots, N_V\}. \tag{5}$$

Let a^j be the activation or hidden layer representation after layer j within the model M. For clarity, we omit j in the following discussion.

Replace intervention. A replace intervention substitutes the original activation a with the scaled feature direction:

$$a' = c \cdot d_i + \epsilon. \tag{6}$$

where d_i is the direction of feature i, c indicates the strength of the intervention, and $\epsilon = N(0, 1)$ is an error term included to find robust causal effects that are resistant against random perturbations. This intervention completely replaces the activation with the feature of interest, allowing us to isolate its effect.

4.2 CAUSAL INTERVENTION

We perform a causal intervention on a using Pearl's do-operator:

$$do(a = a'). \tag{7}$$

This intervention modifies the model M to M' with an intervened activation:

$$P_{M'}(Y|x) = P_M(Y|x, do(a)). \tag{8}$$

By comparing $P_{M'}(Y|x)$ with the original $P_M(Y|x)$, we can assess the causal effect of the intervention on the output.

4.3 DERIVATION FROM GENERAL CAUSAL THEOREM

Starting from the general definition of the Average Causal Effect (ACE) of generating token y given feature d:

$$\text{ACE}(y, d) = \mathbb{E}_{x\sim D}[P_M(Y = y|x, do(a'))] - \mathbb{E}_{x\sim D}[P_M(Y = y|x)], \tag{9}$$

where D is the data distribution. To make the method computationally feasible, we apply the following simplifications:

Zero Baseline Assumption: we assume the following property:

$$\mathbb{E}_{x\sim D}[P_M(Y = y|x)] \approx 0, \tag{10}$$

when y rarely occurs without intervention. This is a valid assumption for tokens that have low prior probability in the model, which is common in large vocabularies.

Monte Carlo Estimation: We perform MC sampling as an estimation of the expectation.

$$\mathbb{E}_{x\sim D}[P_M(Y = y|x, do(a'))] \approx \frac{1}{N}\sum_{i=1}^{N} P_M(Y = y|x_i, do(a')), \tag{11}$$

where N is the number of samples drawn from D. Substituting and simplifying based on our assumptions, we derive the empirical estimate:

$$\text{ACE}(y, d) \approx \frac{1}{N}\sum_{i=1}^{N} P_M(Y = y|x_i, do(a')). \tag{12}$$

For a language model that generates tokens through sampling, we estimate the probability using multiple samples:

$$\text{ACE}(y, d) \approx \frac{1}{NM}\sum_{i=1}^{N}\sum_{j=1}^{M} \mathcal{I}(\hat{y}_j = y|x_i, do(a')), \tag{13}$$

where M is the number of samples per input x_i, $\hat{y}_{i,j}$ is the j-th sampled token for input x_i under intervention, and $\mathcal{I}$ is the indicator function. This metric provides a practical measure to assess the causal role of the feature d in generating token y.

4.4 IDENTIFYING GENERATION FEATURES

We introduce two methods for identifying generation features: the *Single-Token Analysis* and the *Multi-Token Analysis*.

4.4.1 SINGLE-TOKEN ANALYSIS

The *Single-Token Analysis* method aims to identify features that consistently trigger the generation of a single, specific token. A feature d is considered a *generation feature* of token t if:

$$\text{ACE}(t, d) > \tau, \tag{14}$$

where τ is a threshold value.

Clarification on threshold τ: We set default τ to be 0.8 to ensure that the intervention significantly increases the likelihood of generating token t. Specifically, if $\text{ACE}(t, d) > 0.8$, it implies that, on average, the intervention causes the model to generate t more than 80% of the time, indicating a strong causal relationship between feature d and token t.

In practice, evaluating $\text{ACE}(y, d)$ for all tokens $y \in V$ is computationally infeasible due to the large vocabulary size. Therefore, we focus on identifying the most frequently generated token under intervention:

$$y^* = \arg\max_y \left(\frac{1}{NM} \sum_{i=1}^{N} \sum_{j=1}^{M} \mathcal{I}(\hat{y}_j = y | x_i, do(a')) \right). \tag{15}$$

We then check if $\text{ACE}(y^*, d) > \tau$ to determine if feature d is a generation feature for token y^*.

4.4.2 MULTI-TOKEN ANALYSIS

The *Multi-Token Analysis* method extends the *Single-Token method* by accounting for the possibility that a generation feature may correspond to multiple tokens, where the tokens are similar in the embedding space. Instead of looking for a single most frequent token, we analyze the generated sequences to identify a set of closely related tokens that are often triggered by the intervention.

We first obtain the generated sequences of text using the same intervention method as in the *Single-Token Analysis* method. Then, for each generated sequence, we extract the first token. For each sequence, we obtain the embedding vector for the token. These tokens are clustered using a similarity metric. Specifically, we obtain the connected components in the similarity graph formed by connecting tokens based on whether the cosine similarity between their embeddings are greater than a threshold θ. We set the threshold θ to be 0.5. Then, we define the representative set of tokens as the largest connected component found for a feature. This will output a set of tokens and their relative count given an activation. The count is the sum of the number of appearances of each token in the set.

The identified feature is considered a generation feature if the number of tokens in this set appears with the frequency that is greater than a threshold. Let T be the largest cluster (set) of tokens corresponding to feature d, the feature is considered a generation feature if

$$\frac{1}{NM} \sum_{i=1}^{N} \sum_{j=1}^{M} \mathcal{I}(\hat{y}_j \in T | x_i, do(a')) > \tau. \tag{16}$$

In conclusion, we summarize the procedure for identifying generation features in Appendix C.

5 VALIDATION OF GENERATION FEATURE

5.1 EXPERIMENTAL SETUP

Our experiments utilized the `google/gemma-2-2b` (Team et al., 2024) model with SAEs from Gemma Scope (Lieberum et al., 2024), employing the replace intervention method described in Section 4. We focused our analysis on layers 19 through 24, which our preliminary studies indicated contained a higher concentration of generation features. Unless otherwise specified, the SAEs used in our experiments had a width of 16,384 and an average L_0 norm closest to 100. For feature identification, we employed a diverse set of 10 prompts (see Appendix E), generating 10 samples per prompt to ensure robust evaluation. To assess the effectiveness of our approach, we compared our *Single-Token Analysis* method against a baseline inspired by the logit lens technique (nostalgebraist, 2020).

5.2 EVALUATION METRICS

Let F denote the set of identified generation features, where each feature $f \in F$ has an associated target token set t_f (with $|t_f| = 1$ for *Single-Token Analysis*). We define D_{train} as the set of prompts used during feature identification and D_{test} as an independent validation set. The specific prompts used are detailed in Appendix E. We employ two primary metrics for evaluation:

Interventional Score. This metric evaluates the consistency of identified generation features using an independent set of 10 validation prompts D_{self}. For each prompt and feature, we generate 10 samples under feature intervention with strength c. The interventional score for a feature f is defined as:

$$\text{IS}(f) = \sum_{x \in D_{self}} \frac{\sum_{j=1}^{M} \mathcal{I}(\hat{y}_j \in t_f | x, do(a'))}{M}, \tag{17}$$

where $M = 10$ is the number of samples per input, $\hat{y}_j$ is the j-th sampled token under intervention $do(a')$, and $\mathcal{I}$ is the indicator function. The overall interventional score is averaged across features:

$$\text{Interventional Score} = \frac{1}{|F|} \sum_{f \in F} \text{IS}(f). \tag{18}$$

Observational Score. This metric assesses generalizability using activation data from Neuronpedia (Lin, 2023). It measures the likelihood that the model generates (one of) our identified target token(s) if a generation feature is naturally activated. For each feature f, we analyze a set of high activations A_f from Neuronpedia. Each activation $a \in A_f$ corresponds to a token sequence x_a and maximum activating position p_a. The observational score for feature f is:

$$\text{OS}(f) = \frac{\sum_{a \in A_f} \mathcal{I}(t_a \in t_f)}{|A_f|}, \tag{19}$$

where t_a is the token at position $p_a + 1$ in x_a, and $|A_f| = 5$ in our experiments. The overall observational score averages across features:

$$\text{Observational Score} = \frac{1}{|F|} \sum_{f \in F} \text{OS}(f). \tag{20}$$

Baseline method: Our baseline method is inspired by the logit lens (nostalgebraist, 2020). For each feature f, we consider its corresponding decoder weight vector d_f in the sparse autoencoder. We compute the dot product between d_f and the embedding vector e_t for each token t in the vocabulary V. The token t^* with the highest dot product is selected as the baseline's predicted generation token:

$$t^* = \arg\max_{t \in V} (d_f \cdot e_t). \tag{21}$$

We rank features based on the highest dot product value $\max_{t \in V}(d_f \cdot e_t)$. This baseline method is directly comparable to our *Single-Token Analysis* method, as the baseline method identifies a single generation token for the generation features it finds. The precision of the baseline method is computed using the same interventional and observational procedures, substituting $\{t^*\}$ for t_f.

5.3 VALIDATION RESULTS

Tables 1 and 2 present our comprehensive validation results. Table 1 compares the performance of *Single-Token Analysis* and *Multi-Token Analysis* methods across different intervention strengths and thresholds for layers 19-24. Table 2 specifically contrasts our *Single-Token Analysis* method against the baseline approach.

Observations: Table 1 shows that both the *Single-Token Analysis* and *Multi-Token Analysis* methods consistently identify large numbers of generation features. The *Multi-Token Analysis* identifies more features than the *Single-Token Analysis* method. Also, both methods demonstrate a similar performance for interventional scores, with the *Multi-Token Analysis* showing a slightly lower score on observational score, but a significant increase in the number of generation features.

Strength	Threshold	Single-Token Analysis			Multi-Token Analysis		
		# Features	Int. Score	Obs. Score	# Features	Int. Score	Obs. Score
100	0.7	4308	0.868	0.609	6682	0.834	0.574
	0.8	2903	0.916	0.671	4276	0.906	0.651
	0.9	1506	0.953	0.720	2257	0.949	0.718
200	0.7	7748	0.863	0.537	11703	0.852	0.539
	0.8	5165	0.915	0.608	7930	0.907	0.604
	0.9	2707	0.953	0.681	4324	0.949	0.678
300	0.7	9554	0.853	0.496	14655	0.857	0.506
	0.8	6317	0.904	0.561	10013	0.909	0.572
	0.9	3257	0.948	0.642	5526	0.950	0.651

Table 1: Aggregated results for single-token and multi-token analysis from layer 19 to 24.

Str.	Thres.	# Feat.	Ours		Baseline	
			Int.	Obs.	Int.	Obs.
100	0.7	4308	0.868	0.609	0.680	0.512
	0.8	2903	0.916	0.671	0.731	0.568
	0.9	1506	0.953	0.720	0.790	0.621
200	0.7	7748	0.863	0.537	0.530	0.414
	0.8	5165	0.915	0.608	0.595	0.478
	0.9	2707	0.953	0.681	0.683	0.565
300	0.7	9554	0.853	0.496	0.488	0.380
	0.8	6317	0.904	0.561	0.560	0.445
	0.9	3257	0.948	0.642	0.654	0.534

Table 2: Comparison of single-token analysis and baseline. The results are from layers 19 through 24. Our method consistently achieves higher interventional and observational scores.

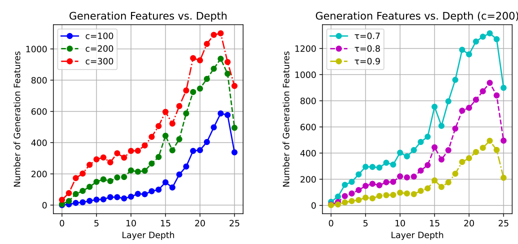

(a) Effect of intervention strength c; Effect of depth

(b) Effect of threshold τ; Effect of depth

Figure 2: Layer-wise distribution of generation features. (a) Variations with different intervention strengths (fixed $\tau = 0.8$); (b) Variations with different thresholds (fixed $c = 200$).

Table 2 demonstrates that our *Single-Token Analysis* method achieves significantly higher interventional and observational scores than the baseline method across all intervention strengths and thresholds, demonstrating the superiority of our causal intervention-based approach for identifying generative neurons compared to a logit lens baseline.

6 GENERATION FEATURES STUDY

6.1 LOCATION OF GENERATION FEATURES

We analyzed the distribution of generation features across different model layers to understand their formation patterns, motivated by recent work on layer specialization (Jin et al., 2025) and layer functionality (Gromov et al., 2025; Zhang et al., 2024). Using the *Single-Token Analysis* method, we examined feature distributions across layers in the `gemma-2-2b` model.

Figure 2 illustrates the layer-wise distribution under varying experimental conditions. Both intervention strength and threshold variations reveal a consistent pattern: generation features become increasingly prevalent in deeper layers, reaching peak concentration in the later layers before showing a slight decline in the final layer. This pattern persists across different parameter settings, suggesting a fundamental aspect of how these models organize generative capabilities.

The increasing density of generation features in later layers aligns with the hierarchical nature of transformer architectures, where deeper layers typically process more abstract and task-specific features. The slight decrease in the final layer may indicate a transition to output-specific processing, where individual feature effects become more diffused.

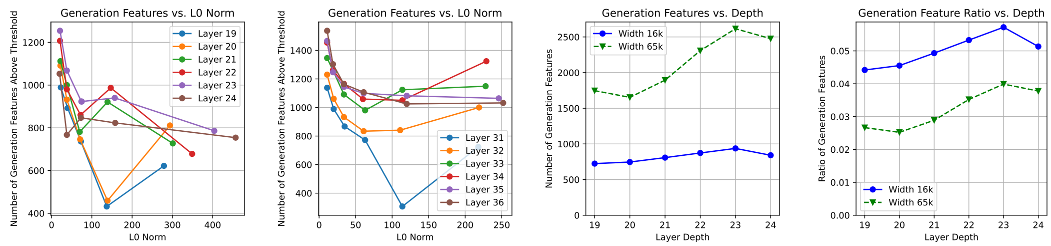

(a) Sparsity study; 2b (b) Sparsity study; 9b (c) Width study; Absolute (d) Width study; Ratio

Figure 3: Impact of SAE sparsity and width. (a) and (b) show generation feature count versus SAE L_0 norm for `gemma-2-2b` and `gemma-2-9b`, respectively. (c) and (d) compare generation features across different SAE widths (absolute count of generation features and ratio of generation features).

6.2 Impact of SAE Sparsity

We investigated the relationship between SAE sparsity and generation feature formation through an ablation study varying the average L_0 norm. The average L_0 norm, representing the average number of non-zero activations in the SAE's hidden layer, directly controls the sparsity level of the learned representations. Prior research suggests that sparsity levels influence feature interpretability and reconstruction quality (Bricken et al., 2023; Chanin et al., 2024), with higher sparsity often yielding more interpretable features despite potential increases in reconstruction loss.

Our analysis focused on layers 19-24 of `gemma-2-2b` and layers 31-36 of `gemma-2-9b`, using SAEs with width 16k, intervention strength $c = 200$, *Single-Token Analysis* and threshold $\tau = 0.8$. As shown in Figure 3a and 3b, for average L_0 norms below 100, we observe a general trend where lower average L_0 norms (higher sparsity) correspond to more identified generation features. This relationship becomes less clear beyond average L_0 norm of 100, where the feature count shows some variability and occasional increases, likely due to the complex interplay between sparsity and feature representation.

The observed pattern in the low average L_0 norm region may be attributed to the feature disentanglement effect of high sparsity, where features are forced to be more distinctive and specialized. In contrast, the variable behavior at higher average L_0 norms suggests that reduced sparsity constraints allow for more complex feature interactions, potentially leading to both feature splitting (a single concept starts to be represented by multiple features) and merging (multiple concepts become encoded in a single feature) phenomena discussed in (Chanin et al., 2024).

6.3 Impact of SAE Width

We examined how SAE width influences generation feature formation by comparing results across layers 19-24 in `gemma-2-2b` for widths of 16k and 65k. Figure 3c and 3d presents this comparison using a fixed intervention strength of $c = 200$ with *Single-Token Analysis* and threshold $\tau = 0.8$.

While the wider 65k SAE identifies more generation features in absolute terms, the ratio of generation features to total width is actually lower compared to the 16k SAE. This suggests that simply increasing SAE width does not proportionally increase the density of generation features. We leave the study of the scaling and explanation of this phenomenon to future research.

6.4 Characteristics of Generation Features

To better understand the nature of identified generation features, we conducted a comprehensive analysis of their distribution and characteristics. Using LLM, we categorized all 1,202 unique generation tokens (corresponding to 10,136 features) into six distinct categories. Table 3 presents this categorization along with representative examples selected from the most frequent tokens within each category, as detailed in Appendix D.2. We also provide the implementation of the categorization in Appendix D.1.

Category	#Tokens	#Features	Example Tokens
Punctuation & Symbols	92	3,794	".", ",", "(", "{", "-"
Common Words & Function Words	189	3,261	"of", "to", "the", "in", "and"
Numbers & Digits	15	256	"0", "1", "2", "4", "3"
Proper Nouns & Named Entities	52	136	"al", "R", "University", "arXiv", "com"
Programming & Code-Related	185	737	"://", "<tr>", "www", "x", "return"
Content Words	669	1,952	"item", "all", "much", "get", "about"

Table 3: Distribution of generation features across categories. Example tokens are selected from the most frequent tokens in each category, as detailed in Appendix D.

Prompt	Feature (Layer, ID)	Original Continuation	Intervention Result
The weather today seems unusually bright and	Layer 22, ID 9836	sunny. I'm not sure if it's because of the time of year...	black. The air is clear as a clear day...
The 44th president of USA is	Layer 25, ID 2222	a man who has been in the limelight for a long time...	Trump. The 44th President is the president of USA...
1+1=	Layer 7, ID 1139	2...	112 - 113 (20 points)...

Table 4: Examples of generation feature interventions. Target tokens to generate are "black", "trump", and "1" from top to bottom. Intervention on one feature at one layer for one token effectively changes the model behavior.

6.5 Examples of Generation Feature Intervention

To demonstrate the practical impact of generation features, we present several examples of how targeted interventions can alter model outputs. Table 4 shows three representative cases where activating specific generation features leads to consistent changes in the model's continuation.

In each case, we observe that activating a specific generation feature (using replace intervention with strength 200) consistently redirects the model's output toward a particular token or concept, regardless of the contextual appropriateness. For instance, in the weather example, activating feature 9836 in layer 22 consistently generates "black" instead of the more contextually appropriate "sunny". This demonstrates how generation features can override context-based generation patterns.

7 Conclusion

In this work, we introduced a novel methodology for identifying and validating generation features—specific sparse autoencoder (SAE) features that reliably control token generation in large language models (LLMs). By systematically applying causal interventions on SAE activations, we demonstrated that these features act as control vectors, consistently influencing the generation of specific tokens or token groups across diverse contexts. Our experiments on the Gemma models revealed that generation features are concentrated in deeper layers, aligning with the hierarchical organization of transformer architectures. We further explored how SAE architectural choices, such as width and sparsity, impact feature interpretability and density, finding that higher sparsity enhances disentanglement while larger widths increase absolute feature counts but lower relative density. Qualitative examples showcased the practical implications of generation features, illustrating their capacity to override contextual outputs and directly control model behavior. These findings provide new insights into the internal organization of LLMs, offering a systematic framework for both understanding and precisely controlling their generative capabilities. While these findings offer promising directions for controlling LLM behavior, they also raise important ethical considerations (see Appendix B). Future work can extend this approach to larger models and explore its applications for fine-grained, interpretable interventions in LLMs while maintaining output coherence and safety.

REFERENCES

Jinze Bai, Shuai Bai, Yunfei Chu, Zeyu Cui, Kai Dang, Xiaodong Deng, Yang Fan, Wenbin Ge, Yu Han, Fei Huang, Binyuan Hui, Luo Ji, Mei Li, Junyang Lin, Runji Lin, Dayiheng Liu, Gao Liu, Chengqiang Lu, Keming Lu, Jianxin Ma, Rui Men, Xingzhang Ren, Xuancheng Ren, Chuanqi Tan, Sinan Tan, Jianhong Tu, Peng Wang, Shijie Wang, Wei Wang, Shengguang Wu, Benfeng Xu, Jin Xu, An Yang, Hao Yang, Jian Yang, Shusheng Yang, Yang Yao, Bowen Yu, Hongyi Yuan, Zheng Yuan, Jianwei Zhang, Xingxuan Zhang, Yichang Zhang, Zhenru Zhang, Chang Zhou, Jingren Zhou, Xiaohuan Zhou, and Tianhang Zhu. Qwen technical report, 2023. URL https://arxiv.org/abs/2309.16609.

Trenton Bricken, Adly Templeton, Joshua Batson, Brian Chen, Adam Jermyn, Tom Conerly, Nick Turner, Cem Anil, Carson Denison, Amanda Askell, Robert Lasenby, Yifan Wu, Shauna Kravec, Nicholas Schiefer, Tim Maxwell, Nicholas Joseph, Zac Hatfield-Dodds, Alex Tamkin, Karina Nguyen, Brayden McLean, Josiah E Burke, Tristan Hume, Shan Carter, Tom Henighan, and Christopher Olah. Towards monosemanticity: Decomposing language models with dictionary learning. *Transformer Circuits Thread*, 2023. https://transformer-circuits.pub/2023/monosemantic-features/index.html.

Tom Brown, Benjamin Mann, Nick Ryder, Melanie Subbiah, Jared D Kaplan, Prafulla Dhariwal, Arvind Neelakantan, Pranav Shyam, Girish Sastry, Amanda Askell, Sandhini Agarwal, Ariel Herbert-Voss, Gretchen Krueger, Tom Henighan, Rewon Child, Aditya Ramesh, Daniel Ziegler, Jeffrey Wu, Clemens Winter, Chris Hesse, Mark Chen, Eric Sigler, Mateusz Litwin, Scott Gray, Benjamin Chess, Jack Clark, Christopher Berner, Sam McCandlish, Alec Radford, Ilya Sutskever, and Dario Amodei. Language models are few-shot learners. In H. Larochelle, M. Ranzato, R. Hadsell, M.F. Balcan, and H. Lin (eds.), *Advances in Neural Information Processing Systems*, volume 33, pp. 1877–1901. Curran Associates, Inc., 2020. URL https://proceedings.neurips.cc/paper_files/paper/2020/file/1457c0d6bfcb4967418bfb8ac142f64a-Paper.pdf.

Yupeng Chang, Xu Wang, Jindong Wang, Yuan Wu, Linyi Yang, Kaijie Zhu, Hao Chen, Xiaoyuan Yi, Cunxiang Wang, Yidong Wang, Wei Ye, Yue Zhang, Yi Chang, Philip S. Yu, Qiang Yang, and Xing Xie. A survey on evaluation of large language models. *ACM Trans. Intell. Syst. Technol.*, 15 (3), March 2024. ISSN 2157-6904. doi: 10.1145/3641289. URL https://doi.org/10.1145/3641289.

David Chanin, James Wilken-Smith, Tomáš Dulka, Hardik Bhatnagar, and Joseph Bloom. A is for absorption: Studying feature splitting and absorption in sparse autoencoders, 2024. URL https://arxiv.org/abs/2409.14507.

Mingda Chen, Qingming Tang, Sam Wiseman, and Kevin Gimpel. A multi-task approach for disentangling syntax and semantics in sentence representations. In Jill Burstein, Christy Doran, and Thamar Solorio (eds.), *Proceedings of the 2019 Conference of the North American Chapter of the Association for Computational Linguistics: Human Language Technologies, Volume 1 (Long and Short Papers)*, pp. 2453–2464, Minneapolis, Minnesota, June 2019. Association for Computational Linguistics. doi: 10.18653/v1/N19-1254. URL https://aclanthology.org/N19-1254/.

Nelson Elhage, Tristan Hume, Catherine Olsson, Nicholas Schiefer, Tom Henighan, Shauna Kravec, Zac Hatfield-Dodds, Robert Lasenby, Dawn Drain, Carol Chen, Roger Grosse, Sam McCandlish, Jared Kaplan, Dario Amodei, Martin Wattenberg, and Christopher Olah. Toy models of superposition. *Transformer Circuits Thread*, 2022.

Leo Gao, Tom Dupre la Tour, Henk Tillman, Gabriel Goh, Rajan Troll, Alec Radford, Ilya Sutskever, Jan Leike, and Jeffrey Wu. Scaling and evaluating sparse autoencoders. In *The Thirteenth International Conference on Learning Representations*, 2025. URL https://openreview.net/forum?id=tcsZt9ZNKD.

Andrey Gromov, Kushal Tirumala, Hassan Shapourian, Paolo Glorioso, and Dan Roberts. The unreasonable ineffectiveness of the deeper layers. In *The Thirteenth International Conference on Learning Representations*, 2025. URL https://openreview.net/forum?id=ngmEcEer8a.

Zhiting Hu, Zichao Yang, Xiaodan Liang, Ruslan Salakhutdinov, and Eric P. Xing. Toward controlled generation of text. In Doina Precup and Yee Whye Teh (eds.), *Proceedings of the 34th International*

Conference on Machine Learning, volume 70 of *Proceedings of Machine Learning Research*, pp. 1587–1596. PMLR, 06–11 Aug 2017. URL https://proceedings.mlr.press/v70/hu17e.html.

Xiaowei Huang, Wenjie Ruan, Wei Huang, Gao Jin, Yizhen Dong, Changshun Wu, Saddek Bensalem, Ronghui Mu, Yi Qi, Xingyu Zhao, Kaiwen Cai, Yanghao Zhang, Sihao Wu, Peipei Xu, Dengyu Wu, André Freitas, and Mustafa A. Mustafa. A survey of safety and trustworthiness of large language models through the lens of verification and validation. *Artif. Intell. Rev.*, 57:175, 2023. URL https://api.semanticscholar.org/CorpusID:258823083.

Robert Huben, Hoagy Cunningham, Logan Riggs Smith, Aidan Ewart, and Lee Sharkey. Sparse autoencoders find highly interpretable features in language models. In *The Twelfth International Conference on Learning Representations*, 2024. URL https://openreview.net/forum?id=F76bwRSLeK.

Ziwei Ji, Nayeon Lee, Rita Frieske, Tiezheng Yu, Dan Su, Yan Xu, Etsuko Ishii, Ye Jin Bang, Andrea Madotto, and Pascale Fung. Survey of hallucination in natural language generation. *ACM Computing Surveys*, 55(12):1–38, March 2023. ISSN 1557-7341. doi: 10.1145/3571730. URL http://dx.doi.org/10.1145/3571730.

Albert Q. Jiang, Alexandre Sablayrolles, Arthur Mensch, Chris Bamford, Devendra Singh Chaplot, Diego de las Casas, Florian Bressand, Gianna Lengyel, Guillaume Lample, Lucile Saulnier, Lélio Renard Lavaud, Marie-Anne Lachaux, Pierre Stock, Teven Le Scao, Thibaut Lavril, Thomas Wang, Timothée Lacroix, and William El Sayed. Mistral 7b, 2023. URL https://arxiv.org/abs/2310.06825.

Mingyu Jin, Qinkai Yu, Jingyuan Huang, Qingcheng Zeng, Zhenting Wang, Wenyue Hua, Haiyan Zhao, Kai Mei, Yanda Meng, Kaize Ding, Fan Yang, Mengnan Du, and Yongfeng Zhang. Exploring concept depth: How large language models acquire knowledge and concept at different layers? In Owen Rambow, Leo Wanner, Marianna Apidianaki, Hend Al-Khalifa, Barbara Di Eugenio, and Steven Schockaert (eds.), *Proceedings of the 31st International Conference on Computational Linguistics*, pp. 558–573, Abu Dhabi, UAE, January 2025. Association for Computational Linguistics. URL https://aclanthology.org/2025.coling-main.37/.

Tom Lieberum, Senthooran Rajamanoharan, Arthur Conmy, Lewis Smith, Nicolas Sonnerat, Vikrant Varma, János Kramár, Anca Dragan, Rohin Shah, and Neel Nanda. Gemma scope: Open sparse autoencoders everywhere all at once on gemma 2, 2024. URL https://arxiv.org/abs/2408.05147.

Johnny Lin. Neuronpedia: Interactive reference and tooling for analyzing neural networks, 2023. URL https://www.neuronpedia.org. Software available from neuronpedia.org.

Kevin Meng, David Bau, Alex Andonian, and Yonatan Belinkov. Locating and editing factual associations in GPT. *Advances in Neural Information Processing Systems*, 36, 2022. arXiv:2202.05262.

nostalgebraist. Interpreting gpt: The logit lens, Aug 2020. URL https://www.lesswrong.com/posts/AcKRB8wDpdaN6v6ru/interpreting-gpt-the-logit-lens.

B. A. Olshausen and D. J. Field. Emergence of simple-cell receptive field properties by learning a sparse code for natural images. *Nature*, 381:607–609, 1996.

JUDEA PEARL. Causal diagrams for empirical research. *Biometrika*, 82(4):669–688, 12 1995. ISSN 0006-3444. doi: 10.1093/biomet/82.4.669. URL https://doi.org/10.1093/biomet/82.4.669.

Senthooran Rajamanoharan, Tom Lieberum, Nicolas Sonnerat, Arthur Conmy, Vikrant Varma, János Kramár, and Neel Nanda. Jumping ahead: Improving reconstruction fidelity with jumprelu sparse autoencoders, 2024. URL https://arxiv.org/abs/2407.14435.

Nina Rimsky, Nick Gabrieli, Julian Schulz, Meg Tong, Evan Hubinger, and Alexander Turner. Steering llama 2 via contrastive activation addition. In Lun-Wei Ku, Andre Martins, and Vivek Srikumar (eds.), *Proceedings of the 62nd Annual Meeting of the Association for Computational Linguistics (Volume 1: Long Papers)*, pp. 15504–15522, Bangkok, Thailand, August

2024. Association for Computational Linguistics. doi: 10.18653/v1/2024.acl-long.828. URL https://aclanthology.org/2024.acl-long.828/.

Nishant Subramani, Nivedita Suresh, and Matthew Peters. Extracting latent steering vectors from pretrained language models. In Smaranda Muresan, Preslav Nakov, and Aline Villavicencio (eds.), *Findings of the Association for Computational Linguistics: ACL 2022*, pp. 566–581, Dublin, Ireland, May 2022. Association for Computational Linguistics. doi: 10.18653/v1/2022.findings-acl.48. URL https://aclanthology.org/2022.findings-acl.48/.

Gemma Team, Morgane Riviere, Shreya Pathak, Pier Giuseppe Sessa, Cassidy Hardin, Surya Bhupatiraju, Léonard Hussenot, Thomas Mesnard, Bobak Shahriari, Alexandre Ramé, Johan Ferret, Peter Liu, Pouya Tafti, Abe Friesen, Michelle Casbon, Sabela Ramos, Ravin Kumar, Charline Le Lan, Sammy Jerome, Anton Tsitsulin, Nino Vieillard, Piotr Stanczyk, Sertan Girgin, Nikola Momchev, Matt Hoffman, Shantanu Thakoor, Jean-Bastien Grill, Behnam Neyshabur, Olivier Bachem, Alanna Walton, Aliaksei Severyn, Alicia Parrish, Aliya Ahmad, Allen Hutchison, Alvin Abdagic, Amanda Carl, Amy Shen, Andy Brock, Andy Coenen, Anthony Laforge, Antonia Paterson, Ben Bastian, Bilal Piot, Bo Wu, Brandon Royal, Charlie Chen, Chintu Kumar, Chris Perry, Chris Welty, Christopher A. Choquette-Choo, Danila Sinopalnikov, David Weinberger, Dimple Vijaykumar, Dominika Rogozińska, Dustin Herbison, Elisa Bandy, Emma Wang, Eric Noland, Erica Moreira, Evan Senter, Evgenii Eltyshev, Francesco Visin, Gabriel Rasskin, Gary Wei, Glenn Cameron, Gus Martins, Hadi Hashemi, Hanna Klimczak-Plucińska, Harleen Batra, Harsh Dhand, Ivan Nardini, Jacinda Mein, Jack Zhou, James Svensson, Jeff Stanway, Jetha Chan, Jin Peng Zhou, Joana Carrasqueira, Joana Iljazi, Jocelyn Becker, Joe Fernandez, Joost van Amersfoort, Josh Gordon, Josh Lipschultz, Josh Newlan, Ju yeong Ji, Kareem Mohamed, Kartikeya Badola, Kat Black, Katie Millican, Keelin McDonell, Kelvin Nguyen, Kiranbir Sodhia, Kish Greene, Lars Lowe Sjoesund, Lauren Usui, Laurent Sifre, Lena Heuermann, Leticia Lago, Lilly McNealus, Livio Baldini Soares, Logan Kilpatrick, Lucas Dixon, Luciano Martins, Machel Reid, Manvinder Singh, Mark Iverson, Martin Görner, Mat Velloso, Mateo Wirth, Matt Davidow, Matt Miller, Matthew Rahtz, Matthew Watson, Meg Risdal, Mehran Kazemi, Michael Moynihan, Ming Zhang, Minsuk Kahng, Minwoo Park, Mofi Rahman, Mohit Khatwani, Natalie Dao, Nenshad Bardoliwalla, Nesh Devanathan, Neta Dumai, Nilay Chauhan, Oscar Wahltinez, Pankil Botarda, Parker Barnes, Paul Barham, Paul Michel, Pengchong Jin, Petko Georgiev, Phil Culliton, Pradeep Kuppala, Ramona Comanescu, Ramona Merhej, Reena Jana, Reza Ardeshir Rokni, Rishabh Agarwal, Ryan Mullins, Samaneh Saadat, Sara Mc Carthy, Sarah Cogan, Sarah Perrin, Sébastien M. R. Arnold, Sebastian Krause, Shengyang Dai, Shruti Garg, Shruti Sheth, Sue Ronstrom, Susan Chan, Timothy Jordan, Ting Yu, Tom Eccles, Tom Hennigan, Tomas Kocisky, Tulsee Doshi, Vihan Jain, Vikas Yadav, Vilobh Meshram, Vishal Dharmadhikari, Warren Barkley, Wei Wei, Wenming Ye, Woohyun Han, Woosuk Kwon, Xiang Xu, Zhe Shen, Zhitao Gong, Zichuan Wei, Victor Cotruta, Phoebe Kirk, Anand Rao, Minh Giang, Ludovic Peran, Tris Warkentin, Eli Collins, Joelle Barral, Zoubin Ghahramani, Raia Hadsell, D. Sculley, Jeanine Banks, Anca Dragan, Slav Petrov, Oriol Vinyals, Jeff Dean, Demis Hassabis, Koray Kavukcuoglu, Clement Farabet, Elena Buchatskaya, Sebastian Borgeaud, Noah Fiedel, Armand Joulin, Kathleen Kenealy, Robert Dadashi, and Alek Andreev. Gemma 2: Improving open language models at a practical size, 2024. URL https://arxiv.org/abs/2408.00118.

Hugo Touvron, Thibaut Lavril, Gautier Izacard, Xavier Martinet, Marie-Anne Lachaux, Timothée Lacroix, Baptiste Rozière, Naman Goyal, Eric Hambro, Faisal Azhar, Aurelien Rodriguez, Armand Joulin, Edouard Grave, and Guillaume Lample. Llama: Open and efficient foundation language models, 2023. URL https://arxiv.org/abs/2302.13971.

Jesse Vig, Sebastian Gehrmann, Yonatan Belinkov, Sharon Qian, Daniel Nevo, Yaron Singer, and Stuart Shieber. Investigating gender bias in language models using causal mediation analysis. In H. Larochelle, M. Ranzato, R. Hadsell, M.F. Balcan, and H. Lin (eds.), *Advances in Neural Information Processing Systems*, volume 33, pp. 12388–12401. Curran Associates, Inc., 2020. URL https://proceedings.neurips.cc/paper_files/paper/2020/file/92650b2e92217715fe312e6fa7b90d82-Paper.pdf.

Yang Zhang, Yawei Li, Xinpeng Wang, Qianli Shen, Barbara Plank, Bernd Bischl, Mina Rezaei, and Kenji Kawaguchi. Finercut: Finer-grained interpretable layer pruning for large language models, 2024. URL https://arxiv.org/abs/2405.18218.

A LIMITATIONS

Our analysis primarily focuses on the Gemma 2 2B model using the Gemma Scope SAE suite (Lieberum et al., 2024), with preliminary experiments on Gemma 2 9B. The generalization of our findings to other model architectures (e.g., LLaMA (Touvron et al., 2023), Mistral (Jiang et al., 2023)) or SAE architecture beyond JumpReLU (Rajamanoharan et al., 2024) used in Gemma Scope remains to be verified.

B POTENTIAL RISKS

The ability to precisely control LLM outputs through generation features, while valuable for research and legitimate applications, carries several potential risks:

- **Adversarial Manipulation**: Generation features could be exploited to override model safeguards or inject unwanted content into model outputs.
- **Bias Amplification**: Targeted activation of certain features might amplify existing biases or introduce new ones into model responses.
- **Misuse in Misinformation**: This technique could be used to force models to generate specific narratives, potentially facilitating the spread of misinformation.

We encourage researchers to carefully consider these risks when building upon this work and to implement appropriate safeguards in practical applications.

C ALGORITHM DETAILS

Algorithm 1 Algorithm for Identifying Generation Features (Replace Intervention)

```
Require: Model M, dataset D, feature directions {d_i}, intervention strength c, threshold τ
Ensure: Set of generation features G
 1: Initialize: G ← ∅
 2: for each feature d_i ∈ {d_i} do                      ▷ Iterate through all feature directions.
 3:     for each sample x ∈ D do                          ▷ Iterate through all samples in the dataset.
 4:         a ← Activation(M, x)                          ▷ Compute the original activation.
 5:         ε ← SampleNoise()                             ▷ Sample noise from N(0, 1).
 6:         a′ ← c · d_i + ε                              ▷ Apply the replace intervention.
 7:         for j = 1 to M do                             ▷ Sample M tokens from the model.
 8:             Sample token ŷ_{x,j} ∼ P_M(Y | x, do(a′))
 9:         end for                                       ▷ Record the frequency of each token generated.
10:     end for
11:     Single-Token Analysis: ▷ Estimate ACE(y, d_i) for each token y using the collected samples.
12:     y* ← arg max_y (ACE(y, d_i))                      ▷ Find token with maximum ACE.
13:     if ACE(y*, d_i) > τ then
14:         Add (d_i, y*) to G
15:     end if
16:     Multi-Token Analysis: ▷ Cluster generated tokens based on embedding similarities to find
        set T.
17:     if (1/NM) ∑_{x∈D} ∑_{j=1}^{M} I(ŷ_{x,j} ∈ T | do(a′)) > τ then
18:         Add (d_i, T) to G
19:     end if
20: end for
21: return G
```

D DETAILED ANALYSIS OF GENERATION FEATURES

D.1 FEATURE CATEGORIZATION METHODOLOGY

We employed the DeepSeek-V2.5 model to categorize generation features using a systematic prompt-based approach. The categorization prompt was structured as follows:

```
Please categorize the following tokens
into one of these categories:
1. Punctuation and Symbols
2. Common Words and Function Words
3. Numbers and Digits
4. Proper Nouns and Named Entities
5. Programming and Code-Related Tokens
6. Content Words

Example categorization:
Input tokens: ["!", "and", "1",
"John", "class", "book"]
Output:
!: 1
and: 2
1: 3
John: 4
class: 5
book: 6
```

D.2 TOP FEATURES BY CATEGORY

Token	Feature Count
.	1,155
,	510
(	370
{	240
-	227
"	109
/	94
;	88
=	83
_	73

Table 5: Top Punctuation & Symbols

Token	Feature Count
of	626
to	488
the	219
in	129
and	109
for	98
as	88
on	71
with	68
from	62

Table 6: Top Common Words & Function Words

Token	Feature Count
0	103
1	59
2	49
4	9
3	7
9	7
5	6
20	4
6	2
7	2

Table 7: Top Numbers & Digits

Token	Feature Count
al	14
R	9
University	8
arXiv	7
com	7
office	7
City	5
Dr	5
God	4
Microsoft	4

Table 8: Top Proper Nouns & Named Entities

Token	Feature Count
://	48
<tr>	27
www	24
x	24
return	21
<tbody>	19
<td>	19
class	18
function	15
php	15

Table 9: Top Programming & Code-Related Tokens

Token	Feature Count
item	24
all	23
much	21
get	20
about	18
new	17
\	16
true	16
public	14
said	13

Table 10: Top Content Words

E Prompts Used for Experiments

E.1 Prompts for Identification

```
prompts:
- "<unk>␣<unk>␣<unk>␣<unk>"
- "He␣finally␣realized␣his"
- "The␣ancient␣library␣held"
- "Whispers␣echoed␣in␣the"
- "They␣raced␣against␣the"
- "Remembering␣the␣days␣when"
- "If␣only␣she␣had␣known"
- "In␣the␣future␣we␣will"
- "The␣door␣creaked␣open,␣revealing"
- "In␣the␣land␣of␣make-believe"
```

E.2 Prompts for Validation

```
prompts:
- "The␣weather␣today␣seems␣unusually␣bright␣and"
- "She␣quickly␣realized␣that␣her␣favorite␣book␣was"
- "By␣the␣time␣the␣concert␣ended,␣the␣crowd"
- "The␣scientist's␣discovery␣led␣to␣a␣groundbreaking"
- "While␣hiking␣through␣the␣forest,␣I␣stumbled␣upon"
- "Despite␣the␣warnings,␣he␣decided␣to"
- "The␣software␣update␣introduced␣several␣new␣features␣that"
- "After␣years␣of␣research,␣the␣team␣concluded␣that"
- "As␣the␣plane␣ascended,␣the␣passengers␣could␣see"
- "He␣always␣wondered␣why␣the␣stars␣seemed␣to"
```